A Review on Recent Progress of Portable Short-Range Noncontact Microwave Radar Systems

Changzhi Li, *Senior Member, IEEE*, Zhengyu Peng, *Student Member, IEEE*, Tien-Yu Huang, *Student Member, IEEE*, Tenglong Fan, Fu-Kang Wang, *Member, IEEE*, Tzyy-Sheng Horng, *Fellow, IEEE*, José-María Muñoz-Ferreras, *Member, IEEE*, Roberto Gómez-García, *Senior Member, IEEE*, Lixin Ran, and Jenshan Lin, *Fellow, IEEE*

(Invited Paper)

***Abstract*— This paper reviews recent progress of portable short-range noncontact microwave radar systems for motion detection, positioning, and imaging applications. With the continuous advancements of modern semiconductor technologies and embedded computing, many functionalities that could only be achieved by bulky radar systems in the past are now integrated into portable devices with integrated circuit chips and printed circuits boards. These portable solutions are able to provide high motion detection sensitivity, excellent signal-to-noise ratio, and satisfactory range detection capability. Assisted by on-board signal processing algorithms, they can play important roles in various areas, such as health and elderly care, veterinary monitoring, human–computer interaction, structural monitoring, indoor tracking, and wind engineering. This paper reviews some system architectures and practical implementations for typical wireless sensing applications. It also discusses potential future developments for the next-generation portable smart radar systems.**

***Index Terms*— Doppler, frequency-modulated continuous wave (FMCW), interferometry, inverse synthetic aperture radar (ISAR), localization, radar, short range, time–frequency.**

I. Introduction

PORTABLE short-range noncontact microwave radar systems with embedded control and communication links have the potential to improve the quality of service in a plurality of areas, such as healthcare, agriculture, infrastructure maintenance, and energy conservation.

Manuscript received October 15, 2016; revised December 29, 2016; accepted December 30, 2016. Date of publication January 30, 2017; date of current version May 4, 2017.

C. Li and Z. Peng are with the Department of Electrical and Computer Engineering, Texas Tech University, Lubbock, TX 79409 USA (e-mail: changzhi.li@ttu.edu; zhengyu.peng@ttu.edu).

T.-Y. Huang and J. Lin are with the Department of Electrical and Computer Engineering, University of Florida, Gainesville, FL 32611 USA (e-mail: tyhuang@ufl.edu; jenshan@ufl.edu).

T. Fan and L. Ran are with the Laboratory of Applied Research on Electromagnetics, Zhejiang University, Hangzhou 310027, China (e-mail: fantl@zju.edu.cn; ranlx@zju.edu.cn).

F.-K. Wang and T.-S. Horng are with the Department of Electrical Engineering, National Sun Yat-Sen University, Kaohsiung 804, Taiwan (e-mail: fkw@mail.ee.nsysu.edu.tw; jason@ee.nsysu.edu.tw).

J.-M. Muñoz-Ferreras and R. Gómez-García are with the Department of Signal Theory and Communications, University of Alcalá, 28871 Alcalá de Henares, Spain (e-mail: jm.munoz@uah.es; roberto.gomezg@uah.es).

Color versions of one or more of the figures in this paper are available online at http://ieeexplore.ieee.org.

Digital Object Identifier 10.1109/TMTT.2017.2650911

By monitoring small mechanical motion and displacement, short-range microwave radars have been investigated for human and animal vital signs detection for a few decades [1]–[10]. Benefiting from the rapid developments of semiconductor technologies, significant advancements in hardware miniaturization and human and animal studies have taken place since the beginning of this century. With focused radiation beams, the technology is further developed into auditory radars for vocal signal detection in applications such as noise rejection, directional discrimination, and remote voice recording [11]–[14]. In cancer radiotherapy, accurate noncontact respiratory monitoring provides a method to dynamically target a tumor with a radiation beam even when the tumor moves due to the respiratory movement of a patient [15]–[17]. On the other hand, being able to sense the mechanical vibration and deflection of building structures enables smart microwave radar sensors for structural health monitoring (SHM) to address worldwide concerns on aging infrastructures [18], [19].

Not limited to the detection of motion waveforms, a time–frequency analysis provides a dynamic way for short-range radars to interpret motion patterns [20], [21], based on which applications including gait analysis, fall detection, gesture characterization, and occupancy sensing have emerged in military and civilian scenarios [22], [23]. In addition, time–frequency analysis of short-range radar signals provides an excellent way to interrogate in real-time the status of rotating structures, which has stimulated the research and application of microwave radar sensors for online monitoring of wind turbine blades [24]–[27]. Technical challenges and solutions in these areas will be discussed.

Another growing area for short-range microwave/millimeter wave radar is precise localization and tracking by measuring distance and angle of arrival [28]–[30]. By transmitting over a bandwidth, frequency-modulated continuous-wave (FMCW) radars and ultrawideband (UWB) radars can accurately localize targets and track their displacements even in a complex indoor environment [31], [32]. Recent advancements for positioning assisted by advanced beamforming and inverse synthetic aperture radar (ISAR) have demonstrated important indoor applications. On the other hand, some innovative multiple-input single-output and multiple-input multiple-output solutions that track moving objects using a few discrete radio frequencies may enhance access to the limited radio spectrum [33]. Although conventional tracking and localization radar sensors were mostly made of large equipment, advanced SiGe/GaN/CMOS technologies, and system methods, such as those exploiting injection locking and six-port architectures, enabled the minimization of tracking and localization radars and significantly broadened their operation frequency range [34], [35].

This paper provides an overview of the recent progress on the development of smart microwave radar systems aided with advanced technologies, such as injection locking, ISAR, flexible electronics, and software-configurable circuits. The scope of applications extends to sleep study, veterinary monitoring and animal study, fall detection, indoor localization, smart house, tumor tracking during cancer treatment, and structure monitoring for civil and wind energy infrastructures. While there are abundant developments on UWB pulsed radar in recent years [36]–[40], this review will be focused on portable continuous-wave (CW) radar systems. It should also be noted that this paper is focused on emerging applications in areas such as biomedical, animal, mechanical, and structural monitoring. While there are many advanced research and applications of 24-GHz and millimeter-wave automotive radar systems, they involve many techniques that are different from the ones reviewed in this paper, and thus are out of scope of this paper. Interested readers are encouraged to refer to [41]–[47].

This paper starts with the fundamental theory of CW radar, including interferometry radar, FMCW radar, and hybrid mode radar in Section II. It then presents application-oriented case studies of motion and displacement monitoring systems in Section III, which also addresses usage of time–frequency analysis for motion sensing systems. Section IV discusses systems with localization and tracking capabilities. Finally, the outlook for portable short-range microwave radar sensing systems will be discussed in Section V.

II. Fundamental Theory of Continuous-Wave Radar

In a basic CW radar system, a known stable-frequency CW radio signal is transmitted, reflected by objects on the radio signal path, and captured by a receiver in the radar system. CW radars can operate in various modes, either unmodulated or modulated. Among them, perhaps the most frequently used ones are the Doppler mode and the FMCW mode.

A. Doppler and Interferometry Radar Systems

Typically, a Doppler radar sends out a single-tone radio signal with frequency f_t. Upon hitting an object, the associated return-signal frequency is shifted away from the transmitted frequency based on the Doppler effect when the object is moving. The backscattered signal frequency f_r received by the radar depends on the speed of light c in the air and the speed v of the target: $f_r = f_t\,(1+v/c)/(1-v/c)$. The Doppler frequency shift is thus $f_d = f_r - f_t = 2vf_t/(c–v)$. Doppler radars are typically used to remotely determine the speed of moving vehicles and to monitor the speed in competition sports, such as golf, tennis, baseball, and NASCAR racing. Because there is no modulation involved and the transmitted signal has a single tone, Doppler radars can be realized at a very low cost.

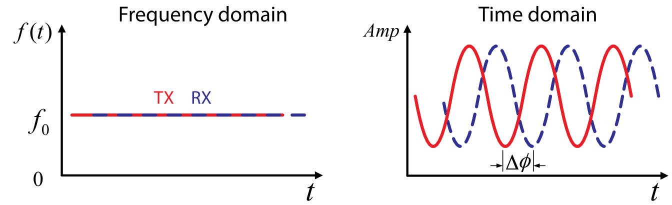

Fig. 1. Interferometry operation for displacement monitoring.

Because signal frequency and phase are related to each other, a similar architecture operating at a single frequency can be used as an interferometry radar to detect the phase change between the transmitted (TX) and received (RX) signals. Interferometry is an important measurement technique in a large variety of fields, such as astronomy, fiber optics, engineering metrology, optical metrology, seismology, spectroscopy, quantum mechanics, remote sensing, biomolecular interactions, surface profiling, microfluidics, mechanical stress/strain measurement and velocimetry, small-displacement measurement, and detection of refractive index changes and surface irregularities [48]. Fig. 1 shows the mechanism for interferometry-radar operation in displacement measurement. The transmitted and received signals have the same frequency, but they have a phase delay $\Delta\phi$ due to the signal propagation path. Without considering the noise and delay associated with the electronic circuitry, $\Delta\phi$ will be proportional to the displacement that is less than $\lambda/2$, where λ is the wavelength. By detecting the change in $\Delta\phi$, the displacement of the target will be determined. The radar receiver uses the same transmitted signal as the local oscillator signal for the down-converter, so that it attains coherent detection with very high displacement detection accuracy. For example, a 2.4-GHz carrier frequency could achieve millimeter-scale displacement measurement accuracy [49].

Doppler and interferometry radars have advantages of simple architecture, narrowband operation, low cost, and can achieve highly accurate speed and displacement measurement. However, they cannot measure absolute distance (i.e., range) of a target.

B. Frequency-Modulated Continuous-Wave Systems

FMCW radars are capable of determining the absolute distance between the system and a target. A variety of modulations for the transmitted signal is possible with the transmitter frequency being able to slew up and down as sine wave, sawtooth wave, triangle wave, or square wave. The basic operation is illustrated in Fig. 2, in which the sawtooth frequency modulation is considered as an example. In this system, the received waveform (RX) is simply a delayed replica of the transmitted waveform (TX). A local copy of the transmitted signal is used to down-convert the received signal to baseband, and the amount of frequency shift Δf between the transmit

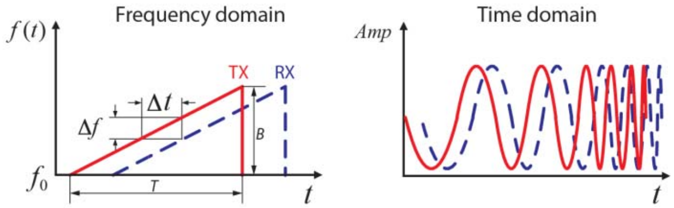

Fig. 2. FMCW operation for range detection.

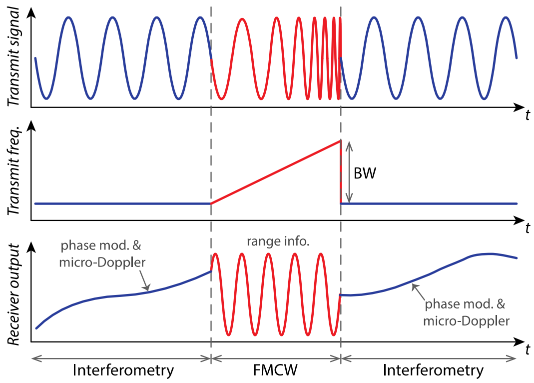

Fig. 3. FMCW-interferometry hybrid operation mode for range and motion measurement.

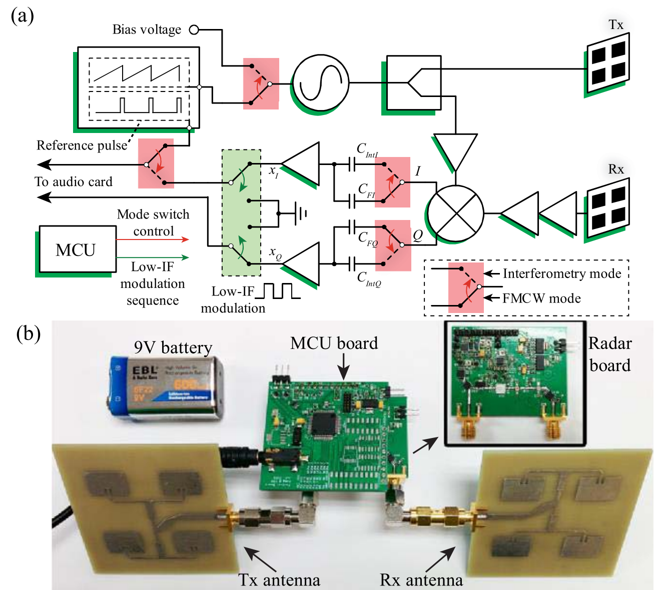

Fig. 4. (a) Block diagram and (b) photograph of a portable FMCW-interferometry hybrid-mode radar system. Adapted from [51].

signal and the reflected signal (i.e., the beat frequency f_b) is linearly proportional to the time delay Δt, leading to $f_b = \Delta t \cdot B/T$, where B is the modulation bandwidth and T is the frequency-modulation sweep time. The range can be thus obtained as $R = c \cdot f_b \cdot T/(2B)$. With the advent of modern electronics, the baseband signal is typically passed through an analog-to-digital converter, and digital processing is performed on the result. The range resolution ΔR of an FMCW radar refers to the minimum separation (in range) of two targets of equal cross section that can be resolved as separate targets, and was found to be proportional to $c/(2B)$. This means that a large modulation bandwidth is needed to achieve a high range resolution. It is worth noting that FMCW radars can extract Doppler information related to the target's velocity, and thus measure displacements of targets if the coherence property of the system is achieved. For example, Wang *et al.* [50] demonstrated tracking of mm-scale human chest wall movements using a linear FMCW radar with a 160-MHz instantaneous transmitted bandwidth centered at 5.8 GHz. However, the hardware and signal processing for an FMCW system to measure displacements are more complex than those of unmodulated CW systems.

C. Hybrid-Mode Radar Systems

The frequency modulation of an FMCW radar can be turned OFF on alternate scans to identify velocity or phase information using an unmodulated radio frequency carrier, which corresponds to Doppler or interferometry mode operation. An example of a hybrid-mode waveform is shown in Fig. 3. This kind of "hybrid-mode" operation allows range and velocity to be found with one radar set. Fig. 4 illustrates an example of a portable 5.8-GHz hybrid-mode radar. In the interferometry mode, the radar transmits a single-tone signal for velocity, displacement, and micro-Doppler measurement. In the FMCW mode, the radar detects absolute range information.

As shown in Fig. 4(a), analog switches configured by an on-board microcontroller are used to set up the radar in one of the two operational modes. For the FMCW operation, the mode switches are turned to solid line in Fig. 4(a) when the voltage-controlled oscillator (VCO) is controlled by a sawtooth-ramp voltage generated by an operational-amplifier-based circuit. The coherence property of the FMCW mode is achieved by using the reference pulse, which is also generated by the operational-amplifier-based circuit, to align the phase of each beat signal. On the other hand, when the radar is changed to the interferometry/Doppler mode, the mode switches are turned to the dash lines in Fig. 4(a) and the VCO generates a single-tone signal. In the receiver, after being amplified by the baseband amplifiers, the signals in the I/Q channels are modulated with a low-IF digital chopping signal, which is realized through the low-IF switches in Fig. 4(a) operated by a microcontroller with a constant frequency. Thus, the mechanical motion signal with low frequencies will be converted to appropriate frequency range that can be digitized by the audio analog-to-digital converter of handheld devices, such as smart phones and laptops.

D. Other Radar Systems

UWB radar systems transmit signals across a wide frequency spectrum that is typically wider than the bandwidth of conventional radar systems [52], [53]. Because the signal energy is spread in a wide bandwidth, the radar signal is usually difficult to detect, leading to low-probability-of-interception capabilities for it. A common technique for modern UWB radar is to transmit pulses with very short durations in nanosecond range or even less. While higher pulse repetition frequencies (PRFs) give rise to a higher number of returned pulses per unit time—and thus improves the average signal quality—lower PRFs avoid range ambiguities that can occur when detection distance is too large.

Instead of transmitting an impulse directly in the time domain, stepped-frequency CW (SFCW) radars synthesize an effective bandwidth in the frequency domain. SFCW radars have been frequently used in ground-penetrating radar applications [54], [55]. In recent years, it has also been investigated for indoor-monitoring tasks, including fall detection and remote human vital signs detection [10], [56]–[58].

Due to the page limit and main focus of the authors' research, this paper will be focused on Doppler, interferometry, FMCW, and hybrid-mode radar. Interested readers are encouraged to refer to papers cited in this section for information on UWB and SFCW radar technologies and applications.

III. Motion and Displacement Monitoring Systems

This section will be focused on portable radar systems for motion and displacement monitoring, without considering acquisition of absolute range. As a result, the radar systems introduced in this section operate on Doppler and interferometry mode, which transmits at one or a few discrete frequencies but has a high motion detection sensitivity due to the coherent phase detection and the range correlation effect [4].

A. Human Vital Signs Detection

By remotely monitoring the signal phase change due to physiological movements, interferometry-mode radars can detect respiration and heartbeat signals without requiring any sensor to be attached to the body. Their areas of exploitation also expand to speech monitoring, as reported at the end of this section. This leads to a large variety of potential applications feasible for these radar sensors, such as sleep study [59]–[61], baby monitors [62], [63], and searching for survivors after earthquake. While the noncontact vital signs detection concept was proposed by pioneers in this field in the twentieth century [1], [2], [64]–[66], research efforts in recent years have been moving the technology toward portable operation, better accuracy, and more robust operation for practical applications.

Furthermore, several studies have demonstrated that the interferometry radar could assist medical linear accelerator (LINAC) in tracking the location of a mobile tumor during lung cancer radiotherapy, to eliminate the side effect due to tumor motion caused by respiratory movement [15], [16], [67]. The challenge for this specific application, however, is the accurate measurement of the movement pattern, which is critical for the radiotherapy dose to be effectively applied to the tumor instead of surrounding healthy tissues. Since the respiratory signal to be detected has a very low frequency and even dc component (i.e., a stationary moment after the end of exhalation), it will be distorted by the coupling capacitor between the mixer and baseband amplifier in the receiving chain. This is illustrated in Fig. 5. Simply connecting the mixer output and baseband amplifier would not help because the baseband circuit may be easily saturated due to the dc offset produced by down-conversion of clutter reflection and TX-to-RX leakage. To resolve the problem, a dc-coupled

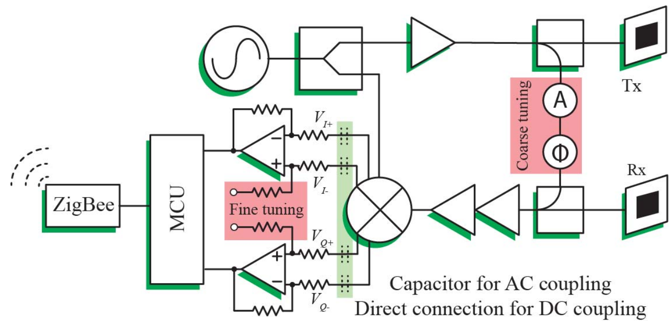

Fig. 5. Block diagram of a 2.4-GHz dc-coupled displacement radar (*iMotion2*) for respiratory monitoring during radiotherapy.

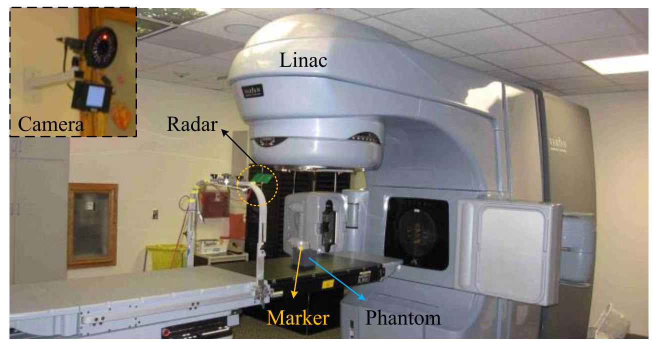

Fig. 6. Experimental setups with a motion phantom measured by a camera and a radar sensor. From [15].

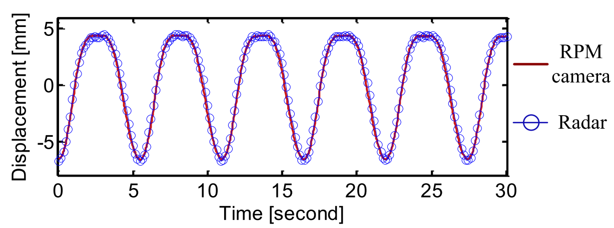

Fig. 7. Phantom motion measured by the radar with the LINAC radiation beam turned ON and comparison with the same phantom motion measured by Varian's RPM system. From [15].

radar with dynamic tuning solution was developed based on a coarse tuning that cancels clutter reflection at the receiver input and a fine tuning that further adjusts the dc bias point of the baseband circuit [15]. A 2.4-GHz portable version of the design is modeled as "iMotion2" and tested on a medical LINAC when the radiation beam is turned ON. Fig. 6 shows the test setup with a motion phantom as the target and an infrared camera to provide the reference. The result in Fig. 7 shows that the radar can precisely measure motion pattern with submillimeter accuracy.

However, the tradeoff found in employing a dc-coupled radar with dynamic tuning is the necessity of monitoring the baseband output dc level and adjust the coarse tuning and fine-tuning in real time, which increases the operation cost. An alternative was recently developed by implementing a postdistortion algorithm to compensate for the frequency-dependent distortion in the baseband output of an ac-coupled radar [68]. The solution can be implemented in software with

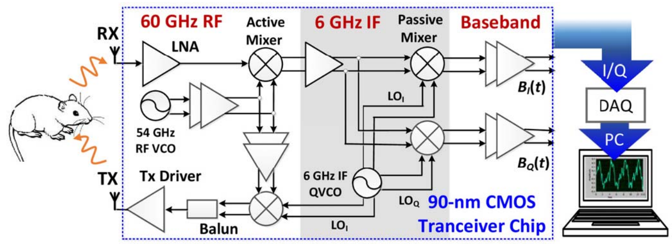

Fig. 8. Experimental setup for measuring cardiorespiratory movement of a laboratory rat using a 60-GHz microradar. From [71] and [72].

a low computational load to enable conventional ac-coupled Doppler radar for accurate movement pattern detection.

B. Veterinary Monitoring and Animal Study

Animal experiments are conducted for various purposes in veterinary medicine, including production and quality control, toxicology and safety tests, and fundamental biomedical research. Most of animal experiments are conducted with mice and rats due to their similarities to human biology, genetic consistency, short lifespan, and quick reproduction [69]. The assessment of cardiorespiratory parameters is crucial in animal testing for studying pathology and developing new treatment. In order to monitor cardiorespiratory activities during animal testing, conventional methods, such as tail-cuff, tether system, indwelling arterial catheter, and implant telemetry, are being used. However, surgical implantation and body-restrained contact also result in increased risk of infection and unintended effect. To overcome the limitations of conventional methods, the technique of using Doppler radar has been proposed. The radar technique can provide noninvasive and noncontact monitoring without the need of cleaning or disposing devices after use. It can reduce animal use by providing long-term monitoring of the same animal and is a useful tool for studying the biological effects in drug development.

The challenge of measuring a small animal's cardiorespiratory activity with radar is its tiny chest wall movement. It is true that millimeter-wave operating frequency (i.e., short wavelength) can be used to increase the sensitivity for detecting small vibrations. However, the strong harmonics caused by the nonlinear Doppler phase demodulation method also complicates the detected spectrum [70]. Although rats have smaller chest-wall displacements compared to humans, the nonlinearity arises in the demodulation process due to the comparable wavelength to the small displacements [70]. By exploiting the harmonics produced by the demodulation method, both frequencies and displacements of both heartbeat and respiration movements of the laboratory rat can be successfully measured [71].

The measurement was performed with a 60 GHz radar [72] to demonstrate the efficacy of noncontact and noninvasive vital sign detection in a laboratory rat. As shown in Fig. 8, the radar was placed in front of the rat housed in a cage, and the sampled I/Q signals [DAQ, 12-b 10 000 sample/s; National Instruments (NI)] were then sent to a computer. Fig. 9(a) shows the radar-measured spectrum of a laboratory rat. To properly choose the demodulation-generated harmonics

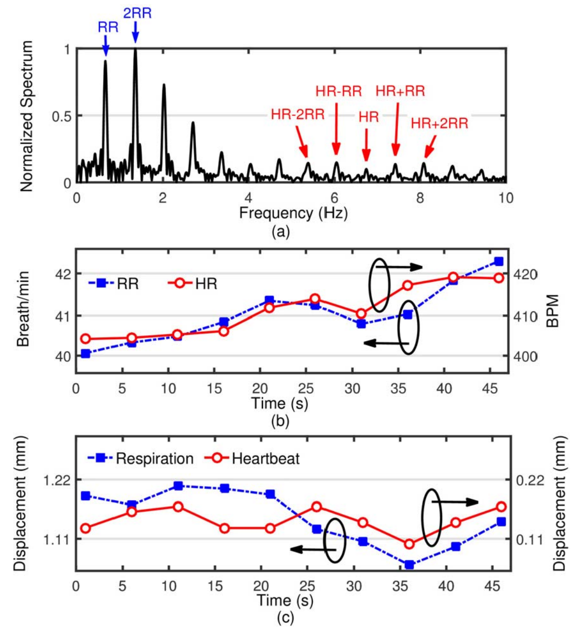

Fig. 9. (a) Radar-measured baseband spectrum of a laboratory rat's vital signs. (b) RR and HR versus time. (c) Displacements of both respiration and heartbeat movements. The figures are replotted from [71].

TABLE I

MEASUREMENT OF A LABORATORY RAT USING RADAR

	Measured Rate	DG Harms Ratio	Calculated m
Respiration	39.6 Breath/min	$\frac{H_{RR}}{H_{2RR}} = \frac{J_1(a_r)}{J_2(a_r)}$	1.19 mm
Heartbeat	403.8 BPM	$\frac{H_{RR}}{H_{HR-RR}} = \frac{J_0(a_h)}{J_1(a_h)}$	0.13 mm

shown on the spectrum, the harmonic-frequency tones produced by the respiration rate (RR) and heart rate (HR) are sorted into two groups to identify the RR and HR and then perform additional data processing to extract displacements [3]. Table I shows the measurement results and calculated displacements of heartbeat and respiratory movements based on Fig. 9(a). The amplitude of harmonics is expressed as H_x, and $J_n(a = 4\pi m/\lambda)$ is the nth-order Bessel function, m is the vibration displacement, and a_h and a_r represent heartbeat and respiration coefficients, respectively. Fig. 9(b) and (c) shows the variations of frequencies and displacements, respectively, in a 47 s recording time period. The experimental results clearly show the cardiorespiratory activities of a lab animal using microwave radar, which provides useful information without using implant devices. In addition to the measured RR and HR, the calculated displacement can be used to construct an adaptive harmonics cancellation technique to enhance the accuracy of heartbeat detection [73].

Recently, self-injection locked (SIL) radar has garnered attention due to its high sensitivity to vital sign detection [74], [75]. In its basic operation, a VCO transmits a CW signal, which is partially reflected by a distant biological

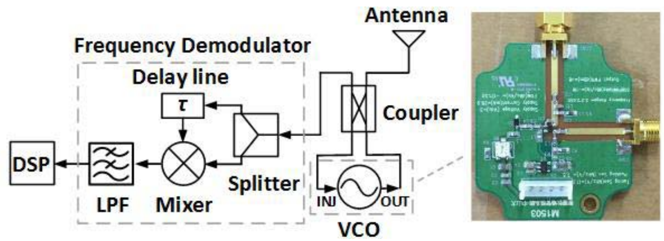

Fig. 10. Block diagram of a prototype SIL radar system.

object, and then injected into the same VCO to form an SIL state. The Doppler modulation that is related to the object's physiological movement can be simply extracted by frequency demodulation of the oscillator output. Since there is no mixing between RF and local oscillator signals in the reception process, the SIL radar is inherently immune to stationary clutter, such as that produced by background reflection and antenna coupling. Due to this advantage, the SIL radar has attracted great interest from the livestock industry and is actively being exploited to monitor animal health in harsh backscattering environments, such as the monitoring of cow's vital signs in a barn where metallic fences are largely used. Furthermore, the SIL radar uses a single antenna to transmit the CW signal and then receive the echo signal without the need to isolate both signals. This benefit avoids the trouble of setting up two antennas, particularly two high-gain antennas.

Fig. 10 shows the block diagram of a prototype SIL radar system that was built for licensing to dairy companies. The system, operating at 2.4-GHz ISM band, comprises an antenna, a VCO with an injection terminal, a coupler, a frequency demodulator that is composed of a splitter, a passive mixer, a delay line and a lowpass filter, and a digital signal processing (DSP) unit. In the RF circuit of this system whose photograph is shown in Fig. 10, the VCO is the only active component while the others are the passive coaxial components from commercial off-the-shelf products. This VCO, fabricated on an FR4 substrate, uses a Clapp configuration along with an injection port connected to the gate of the transistor. It has a tuning range from 2.3 to 2.65 GHz and an output power level of 5 dBm under a power consumption of 140 mW. All the RF circuit components are housed together in a rugged metallic box for protection from cow manure splash.

In health monitoring for cows, RR and pulse rate are important because they tell if cows are feverish, or hot or normal. To measure these two rates, the antenna beams are empirically directed to the belly and neck of the cow as shown in Fig. 11(a) and (b), where the movements caused by the respiration and the carotid artery pulse, respectively, are most significant. In Fig. 11(a) and (b), a high-gain antenna of 18 dBi was used for the radar system to detect RR or pulse rate at one meter away from the cow. The RF processing yields a Doppler signal that is associated with the movement of the antenna's illumination area on the cow. Following further DSP operation, the time–frequency spectrogram of the signal is constructed and used to identify the respiration or pulse frequency when the cow is stationary. Then, a bandpass moving average filter

(a) (b)

Fig. 11. Detection of vital signs on different areas of a cow. (a) Belly. (b) Neck.

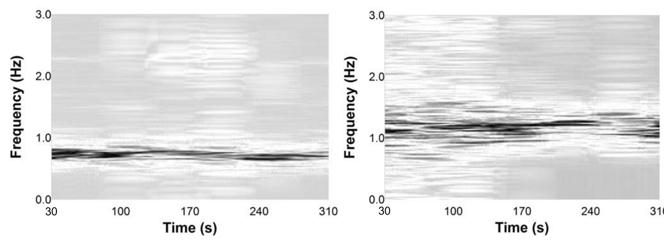

(a) (b)

Fig. 12. Spectrograms with bandpass moving average filtering to enhance the vital sign frequencies of the cow. (a) Respiration. (b) Pulse.

is employed to emphasize the spectrogram at the identified frequency [9], as illustrated by the results shown in Fig. 12(a) and (b) for the measurement on the belly and neck, respectively, of the cow. In Fig. 12(a) and (b), the diffusion phenomena of the target frequency lines are mainly caused by the residual motion artifacts after filtering. Nevertheless, a frequency line of about 0.75 and 1.2 Hz, corresponding to an RR of 45 beats/min and a pulse rate of 72 beats/min, respectively, is observed in the figures over a period of 280 s. The pulse frequency line is more diffuse than the respiration one because the neck moves more greatly and frequently than the belly. It is noted that the obtained RR and pulse rate of the cow from the radar system were verified by a veterinary using a stethoscope on the chest area of the cow.

Doppler radar has also been applied to monitor the health and behavior of other animals, including lizards and fish. Interested readers are referred to [76]–[78] for details.

C. Structural Vibration Monitoring

Aging of infrastructure has raised worldwide concerns. Multiple sensing solutions are being investigated to provide continuous SHM [79]. For example, accelerometers have been used for vibration measurement, but they suffer from degraded performance for slow movements and displacements [80], [81]. Contact displacement sensors, such as linear variable differential transformers, provide accurate measurements but require attachment to a fixed reference point, leading

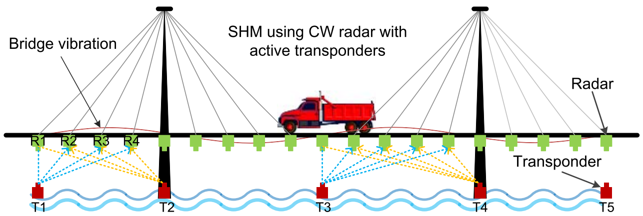

Fig. 13. Concept of using a distributed radar sensor network to monitor the vibration and deflection of a long span bridge.

Fig. 14. (a) Experimental setup of the full-scale bridge test at O'Leno State Park in Florida, USA. (b) 2.4-GHz DC-coupled radar enclosure with an accelerometer and the transponder. From [19].

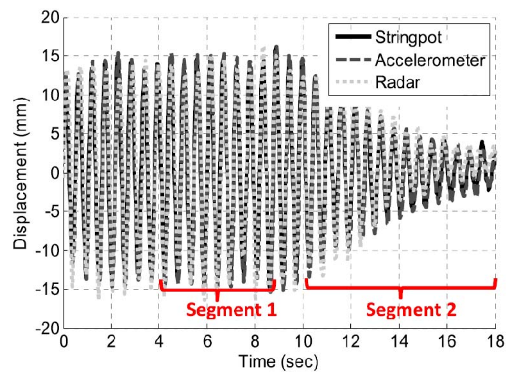

Fig. 15. Time history record of displacement measurement results from all the sensors. From [19].

to complex installation setup that is not suitable for most field applications [82]. CW radar sensors are a promising technology for displacement and vibration measurements for SHM, as the previous sections have already demonstrated the capability of high accuracy noncontact measurement for slow movement. Some researchers have used noncontact microwave interferometers to measure the displacement vibration response of a steel plate girder bridge [82]. The sensors consisted of a 61 cm parabolic dish placed under the bridge and pointing back to a portion of the underside of a single plate girder, with the cost of each prototype at U.S. $1000 in 1997. Other researchers tried to use radar-based sensors to measure structural deflections, but the solution uses complex hardware with very high sampling rates [83]–[85]. In addition, the system could not differentiate targets at the same distance (i.e., no cross-range resolution) due to the backscattering detection mechanism.

To solve the problem of backscattering radar, recently researchers proposed implementing portable radar sensors along a bridge, and use active transponders under a bridge as reference points, to precisely track the vibration and displacement for each critical point on the bridge. An implementation block diagram is shown in Fig. 13. Compared with passive backscattering, the active transponder configuration is capable of increasing the power or changing the frequency of signals reflected from reference points, thereby significantly suppressing the influence of undesired reflection from surrounding clutter (e.g., moving objects near the bridge). Because clutter reflection is mitigated, it also significantly relaxes the requirement on antenna directivity, thus making SHM possible using miniaturized radar sensors that operate in GHz range for longer operation range and lower cost compared with millimeter-wave radar sensors.

A series of laboratory experiments to demonstrate the performance of the transponder configuration has been conducted in [19]. The investigation revealed that the signal improvement provided by the transponder is a function of the distance between the transponder and the radar. In addition, a full-scale bridge test was conducted at the O'Leno State Park in Florida, USA, which is shown in Fig. 14. The test was set up at the quarter span of the bridge directly over one of the embankments. The radar was housed in a weatherproof enclosure and attached to the bottom side of the beam with its antenna facing toward the ground surface. A transponder was placed 248 cm from the radar on the ground directly below the radar. To validate the measurements obtained from the radar/transponder, a string potentiometer and a single-axis accelerometer (PCB Piezotronics, 1000 mV/g sensitivity, sampled at 500 Hz) were installed at the same location. One end of the string potentiometer was connected to the radar enclosure, and the other end was attached to the tripod hosting the transponder. The bridge was excited by a person jumping at a location close to the quarter span, with a frequency close to the first natural frequency of the bridge. All the sensors simultaneously measured the resulting vertical motion of the bridge at the quarter span.

The displacement measurement results are shown in Fig. 15. The result from the accelerometer was obtained by double-integrating the measured acceleration and passing the results to an equiripple finite-impulse response high-pass filter with a cutoff frequency of 0.1 Hz. Otherwise, the low-frequency noise of the accelerometer would be amplified during the integration process. With the help from the transponder, the dc-coupled radar successfully measured both the constant amplitude motion (segment 1, less than 1 mm error) and the decaying amplitude motion part (segment 2, less than 2 mm error) of the bridge vibration, in comparison with the other sensors. On the other hand, when the transponder is turned OFF, the radar working in passive scattering mode was unable to reliably measure the motion. It should be noted that, due to practical nonidealities such as insufficient suppression of

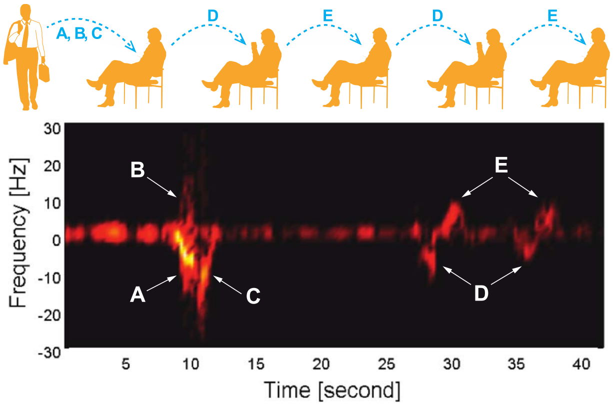

Fig. 16. Micro-Doppler information when a person sat down (A, B, C) and waived hands twice (D, E). Adapted from [90].

clutter noise, although the full-scale bridge test successfully demonstrated the advantage of active transponder mode of portable radar for SHM, it did not confirm previous lab results showing potential advantages of radar sensors over accelerometers [86]. Continuing efforts are then needed from industrial and academic researchers to further improve the performance. Potential research areas in this context include increasing the detection range, reducing beamwidth without increasing antenna size, and developing frequency-conversion transponders that will have better clutter/noise rejection.

D. Gesture Characterization Using Time–Frequency Analysis

Time–frequency analysis studies a signal over both time and frequency by mapping a 1-D signal into a 2-D representation of energy versus time and frequency. Analysis of the radar-detected signal in both time and frequency domains can reveal features of a movement for classification purposes [20], [21], [87], [88]. Especially, local mechanical vibrations or rotations of a target or part of a target may induce additional frequency modulations as a function of time, causing the micro-Doppler effect [89]. For example, Fig. 16 shows the micro-Doppler when a person sat down, and raise and put down one hand twice [90]. Original research in this area was mainly based on relatively bulky bench top radar systems or modules. In recent years, because of the advancements of semiconductor technologies and embedded computation, it became possible to use small portable radar devices to analyze motion features in time–frequency domain for the Internet of Things (IoTs) applications. In one example [91], a portable smart radar gesture recognition sensor achieved 96.7% accuracy for identifying different types of hand movements and head movements. The device was able to differentiate hand lifting and hand pushing based on four features extracted from the measured results. Not only academia, but the information technology industry is also working on gesture recognition using integrated devices for IoT applications. In May 2015, Google launched to public the project *Soli*, which aims to develop robust, high-resolution, and low-power miniature gesture sensing technology for human–computer interaction based on millimeter-wave radar [23]. The team's solution was based on an integrated millimeter-wave radar sensor chip, a high temporal resolution gesture tracking, a hardware abstraction layer, interaction models, and gesture vocabularies. Demonstration showed a submillimeter accuracy and a speed of 10 000 frames/s on embedded hardware. Other companies are also investigating applications of radar-based gesture characterization. For example, NVIDIA Research developed a short-range FMCW monopulse radar for hand-gesture sensing as a key element in intelligent driver assistance systems [92].

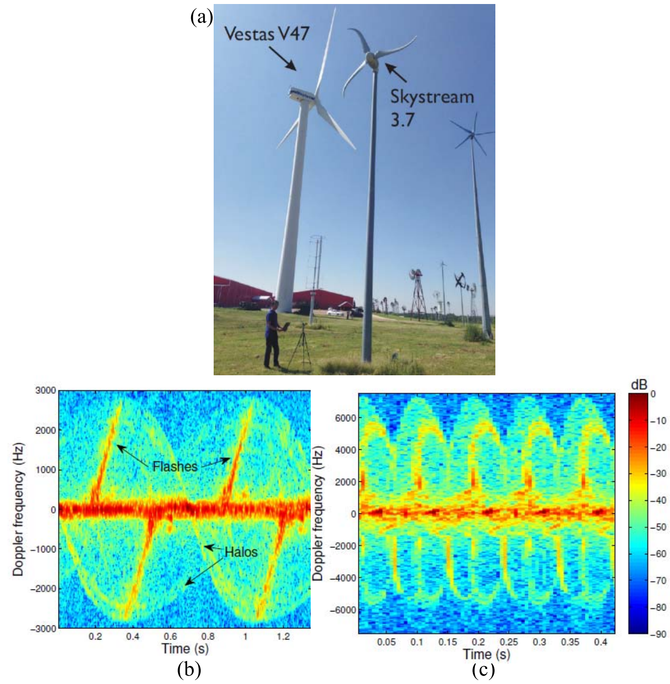

Fig. 17. (a) Using portable radar to measure a Vestas V47 wind turbine with straight blades and a Skystream 3.7 wind turbine with curved blades. (b) Time–frequency signature of Vestas V47 turbine blades measured by a C-band radar. (c) Time–frequency signature of Skystream 3.7 turbine blades measured by a K-band radar. From [26].

E. Turbine Blade Monitoring

As wind turbines increase in size and cost, there is a growing need for early detection of structural and mechanical problems to avoid further damage. It is shown that blade damage is the most expensive one to repair and has the longest repair time [93]. Without prompt correction, rotating mass unbalance due to minor blade damage can also cause serious secondary damage to the system. Common detection methods for rotor imbalance examine variation in rotor speed and transverse oscillations of the nacelle [94]. The acoustic emission method is used during laboratory fatigue cycle tests of blades [95]. Optical systems have been developed for delineating the global shape of large blades [96] while fiber-optical sensors are embedded in wind turbine blades and collect information regarding strain, temperature, and curvature [97].

As a noncontact solution, low-cost low-profile radars are gaining interest for providing real-time structural information on a large number of wind turbines. Using time–frequency analysis, Doppler features can be investigated for each blade while a turbine is running [24], [25]. Fig. 17 shows an example

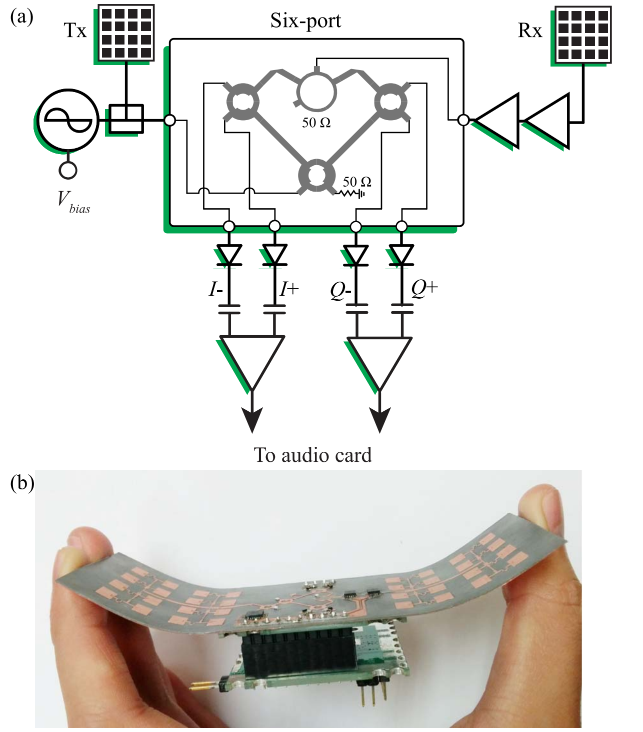

Fig. 18. (a) Block diagram and (b) photograph of a 24-GHz radar on flexible substrate for monitoring of wind turbine blades.

using 5.8- and 24-GHz portable radar sensors to monitor wind turbines in the American Wind Power Center, Lubbock, TX, USA [26]. The 5.8-GHz radar is the hybrid mode radar discussed in Fig. 4 operating in the Doppler mode, whereas the 24-GHz radar is shown in Fig. 18. Two different turbines were measured: a 660-kW Vestas V47 wind turbine with a 47-m rotor diameter and a 1.9-kW Skystream 3.7 wind turbine with a 3.7-m rotor diameter. It should be noted that the Vestas V47 turbine has straight blades while the Skystream 3.7 turbine has curved blades. On the returned spectrograms in Fig. 17(b) and (c), it is clearly shown that different blade shapes induced different features for the spectrogram flashes, verifying the feasibility to monitor the shape and distortion of turbine blades with low-cost portable radar sensors while a turbine is operating. Interested readers are referred to [26] for detailed discussions on practical issues, such as the optimal acquisition angle, the generation of flashes on the spectrogram, the correspondence between the flash shape and the blade shape, the effect of energetic scatterer, and the effect of I/Q mismatch in the portable radar.

F. Other System Realizations and Applications

Taking advantage of the millimeter or submillimeter sensitivity that can be easily achieved using GHz-range Doppler/interferometry radars, many more applications have emerged with the help of various back-end signal processing methods proposed in recent years. For example, Wang *et al.* [98] used an extended differentiate and cross-multiply algorithm to demodulate the detected baseband signal and recover the original vibration information, enabling the

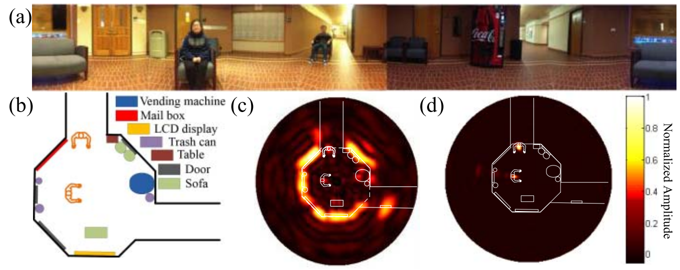

Fig. 19. Indoor positioning and human identification. (a) Experiment setup. (b) Room layout. (c) 2-D positioning map obtained in FMCW detection mode. (d) Result of human tracking based on vital signs. Adapted from [90].

detection of a failure (i.e., undesired speed change) in a mechanical vibration with 12-mm amplitude. Using time–frequency analysis [14] and a variational mode decomposition-based algorithm [12], directional discrimination, background noise rejection, and vocal folds vibration detection were realized for portable auditory radars. In two high-sensitivity radar design competitions held in the International Microwave Symposium in 2014 and 2015, researchers from multiple countries have demonstrated various portable low-power motion detection radars covering a broad frequency range from 2.4 to 80 GHz. The designs of two teams can be found in [99] and [100].

IV. Localization and Tracking Systems

A. Indoor 2-D Mapping Using FMCW and Hybrid Systems

The FMCW-interferometry hybrid mode works in a "burst-FMCW" fashion, where short-time range spectrum analysis can be carried out for a single FMCW chirp in an embedded digital signal processor, thus obtaining satisfactory range estimation with a good signal-to-noise ratio. By pointing a portable device to different directions or steering its signal beam electronically, capability to map an indoor environment would be enabled. On the other hand, the interferometry mode offers very high motion detection sensitivity (i.e., millimeter or submillimeter motion detection sensitivity with GHz carrier signals) at a low computational load, which facilitates activity monitoring. Fig. 19 shows a demonstration of 2-D human-aware indoor mapping based on this idea [90]. With FMCW operation, the hybrid radar can detect the hallway layout with both furniture and human targets as shown in Fig. 19(c). The interferometry mode together with deramping-based FMCW analysis can differentiate between humans and other objects based on physiological motion, and thus identify the human targets as shown in Fig. 19(d) [90]. Although the result of Fig. 19 was obtained from a system including a desktop NI PXI-based signal generator, similar localization and human identification results can be obtained using portable devices such as the 5.8 GHz hybrid-mode radar shown in Fig. 4.

B. Range-Doppler Tracking and Fall Detection

ISAR is a radar technique based on a 2-D high-resolution image to track a target [101]–[103]. ISAR images are often produced by rotating the target and processing the resultant

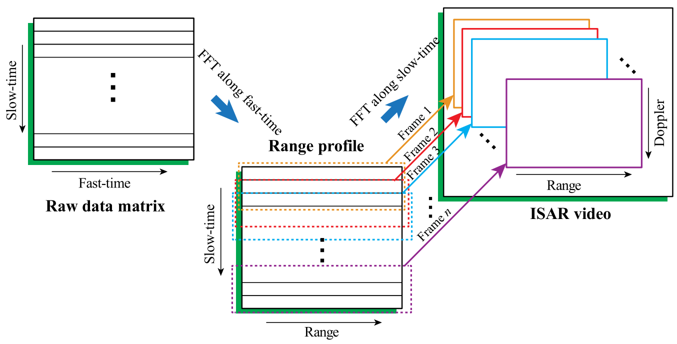

Fig. 20. Generation of range-Doppler ISAR video based on two fast Fourier transforms to the original radar-detected signal.

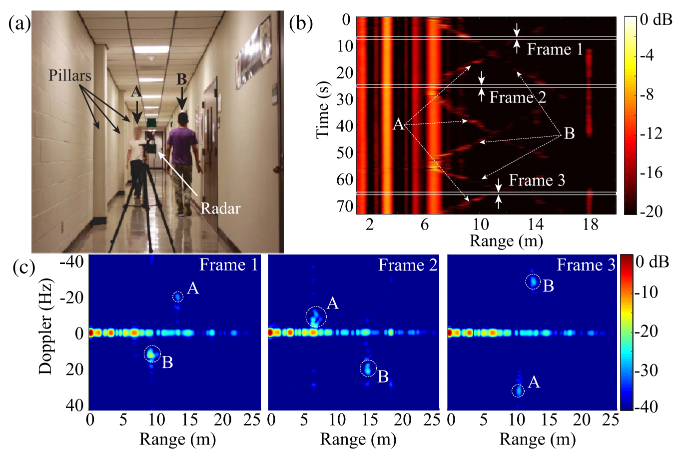

Fig. 21. (a) Experimental setup for ISAR tracking of multiple walking subjects. (b) Range-profile matrix. (c) ISAR video frames at different moments. Adapted from [51].

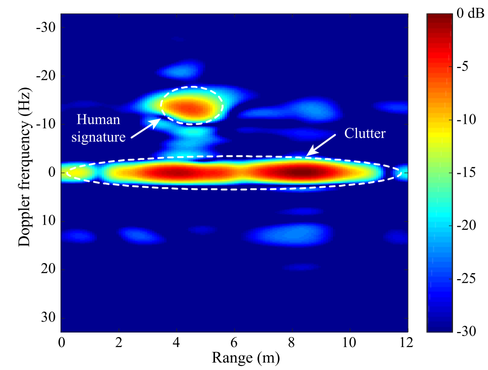

Fig. 22. ISAR image of a walking subject with increased limb motion, which creates abundance of information due to the micro-Doppler effect.

Doppler histories of the scattering centers. The same principle of analyzing Doppler histories of a target at a given range can be used for indoor tracking. The mechanism is shown in Fig. 20. A coherent FMCW radar detects a signal that can be arranged in a slow-time versus fast-time matrix. Performing Fourier transform along the fast-time finds the beat frequency, which converts the fast-time information into range information. After that, the range-profile history is divided into running windows along the slow time. Performing Fourier transform along the slow time for each window converts the slow-time range variation into Doppler information. As a result, a series of range-Doppler history can be obtained for the running windows, which can form an “ISAR video.” It should be noted that the ISAR video discussed in this paper is different from a conventional ISAR image: ISAR image requires rotating the target to illustrate the detailed profile of a target, whereas the ISAR video used in this section can differentiate moving targets in the range-Doppler domain even if they are moving linearly without any rotation.

An example using the 5.8-GHz portable radar is given in Fig. 21, where two human subjects walked back and forth in opposite directions in a narrow corridor. The radar-detected range-profile in a 73-s interval is shown in Fig. 21(b). Many strong vertical strips, which correspond to stationary objects, can be observed. Although the traces of the two moving human subjects are noticeable as indicated by A and B, they are much weaker than the stationary clutter (i.e., nearby objects) returns. Fig. 21(c) plots three frames of the real-time ISAR video obtained by processing the same measurement data. The range information is indicated in the x-axis and the Doppler information (corresponding to walking speed) is indicated in the y-axis. Frame 1 corresponds to the 7-s moment of the acquisition time, when subject A was walking toward the radar, while subject B was walking away from the radar. The return associated with subject A appears above the zero-Doppler strip, while subject B provides an echo below the zero-Doppler signature. In Frame 2 corresponding to the 26-s instant, subject A was close to the radar and was about to turn around with a near-zero velocity, while subject B was still walking away from the radar system. Frame 3 taken at the 64-s moment shows subject A walking back to the radar and subject B walking away from the radar. The echoes observed around the main signatures in these frames correspond to the micro-Doppler features of the human gaits, which were mainly caused by relative limb motion.

It should be noted that all the stationary clutter returns in a complex indoor environment are compressed into the zero-Doppler line in an ISAR video. This leads to the advantage of easy isolation of the wanted moving targets from surrounding clutter. Furthermore, by analyzing the echoes in the ISAR image and the micro-Doppler features of human motion, gait information and fall events can be detected. An example is given in Fig. 22, where a single subject was walking with increased limb motion. It is clearly shown that the echo is defocused and more micro-Doppler features are produced. From the ISAR video, the speed, range, and radar cross section (RCS) can all be observed in real time, which provides possibility of classifying human motions and detect falling of a person. In [104], a case study was conducted to demonstrate the ability of a 5.8-GHz portable FMCW radar sensor to detect fall events and differentiate falls from other activities, such as a sudden jump based on the Doppler, range, and RCS extracted from real-time ISAR imaging.

C. Hand Tracking and Gesture Recognition Using SIMO

In addition to gesture characterizations based on time–frequency analysis and “micro-Doppler” effect, linear time-domain motion tracking based on CW radar sensors can

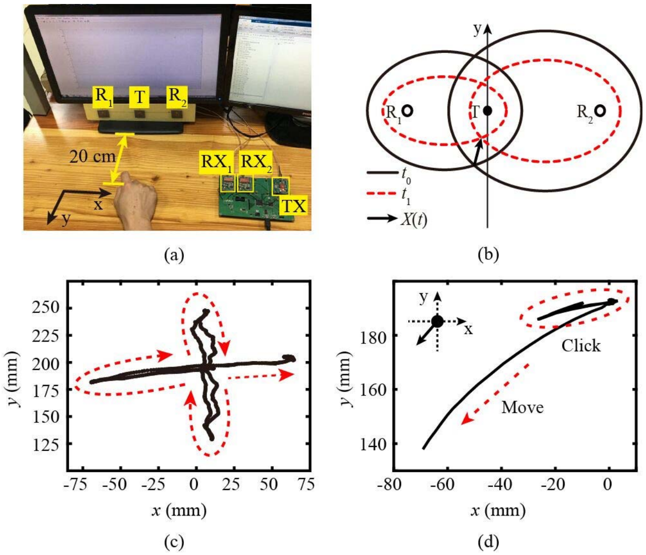

Fig. 23. (a) Experimental setup for hand location and finger gesture tracking. (b) Geometrical interpretation of the problem. (c) Measured hand movement in the x- and y-directions. (d) Finger click measured together with hand movement. Adapted from [106].

also be used in hand tracking, gesture classification, and recognition. A recent example was reported in [105] and [106], where the feasibility of human hand gesture recognition was investigated. This paper tried to realize the basic "moving" and "click" functions of a mouse by remotely tracking the hand and finger actions based on a single-input multiple-output (SIMO) Doppler radar sensor.

The experiment setup is shown in Fig. 23(a). The SIMO system consists of one transmitting and two receiving channels designed to operate at 5.8 GHz. The antennas were placed on the lower side of a computer's display to detect the hand actions in front of them. For a hand moving on the surface of the desktop, a 2-D motion tracking algorithm can be derived by locating the point intersected by the desk surface and the surfaces of two ellipsoids with focuses at the locations of the antennas, as shown in Fig. 23(b). It turned out that when the transmitting and receiving antennas were placed in a straight line parallel to the desktop, two simple equations can be derived to track the trajectory of the hand motion based on the Doppler information demodulated from the scattered signal using an arcsine algorithm. As an experimental demonstration, Fig. 23(c) and (d) shows the reconstructed cross-motion pattern and the moving-click pattern of a hand moving on the desk surface.

These results imply that hand tracking and gesture recognition can be realized using a narrowband signal with the aid of multiple receivers or transmitters, providing a way of enhancing access to the limited radio spectrum.

V. Conclusion

Driven by the need of improved applications on the areas of healthcare, automotive navigation, and smart human–computer interface, the past decade has witnessed rapid advancements in radio frequency sensing and detection technologies. This paper reviews some of the recent developments on portable CW radar systems for short-range applications that are based on sensing of motion, displacement, and location. Although lots of progress has been made by engineers and researchers to minimize radar sensors and make them "smart" for IoT applications, the adoption of radar sensors in daily civilian life is still greatly lagging behind other technologies, such as cameras and accelerometers. With radar's unique advantage of being able to see-through-the-wall and better protect privacy compared with cameras, the microwave society should be optimistic about the potential and future of portable radar sensing technology. The continued contributions from the members in the RF/microwave society will be greatly valued and appreciated.

References

[1] J. C. Lin, "Noninvasive microwave measurement of respiration," *Proc. IEEE*, vol. 63, no. 10, p. 1530, Oct. 1975.

[2] J. C. Lin, "Microwave sensing of physiological movement and volume change: A review," *Bioelectromagnetics*, vol. 13, no. 6, pp. 557–565, 1992.

[3] A. D. Droitcour, O. Boric-Lubecke, V. M. Lubecke, and J. Lin, "0.25 μm CMOS and BiCMOS single-chip direct-conversion Doppler radars for remote sensing of vital signs," in *IEEE Int. Solid-State Circuits Conf. (ISSCC) Dig. Tech. Papers.*, vol. 1. Feb. 2002, pp. 348–349.

[4] A. D. Droitcour, O. Boric-Lubecke, V. M. Lubecke, J. Lin, and G. T. A. Kovacs, "Range correlation and I/Q performance benefits in single-chip silicon Doppler radars for noncontact cardiopulmonary monitoring," *IEEE Trans. Microw. Theory Techn.*, vol. 52, no. 3, pp. 838–848, Mar. 2004.

[5] Y. Xiao, J. Lin, O. Boric-Lubecke, and V. M. Lubecke, "Frequency-tuning technique for remote detection of heartbeat and respiration using low-power double-sideband transmission in the Ka-band," *IEEE Trans. Microw. Theory Techn.*, vol. 54, no. 5, pp. 2023–2032, May 2006.

[6] B.-K. Park, O. Boric-Lubecke, and V. M. Lubecke, "Arctangent demodulation with DC offset compensation in quadrature Doppler radar receiver systems," *IEEE Trans. Microw. Theory Techn.*, vol. 55, no. 5, pp. 1073–1079, May 2007.

[7] C. Li, V. M. Lubecke, O. Boric-Lubecke, and J. Lin, "A review on recent advances in Doppler radar sensors for noncontact healthcare monitoring," *IEEE Trans. Microw. Theory Techn.*, vol. 61, no. 5, pp. 2046–2060, May 2013.

[8] G. Vinci *et al.*, "Six-port radar sensor for remote respiration rate and heartbeat vital-sign monitoring," *IEEE Trans. Microw. Theory Techn.*, vol. 61, no. 5, pp. 2093–2100, May 2013.

[9] F. K. Wang, Y. R. Chou, Y. C. Chiu, and T. S. Horng, "Chest-worn health monitor based on a bistatic self-injection-locked radar," *IEEE Trans. Biomed. Eng.*, vol. 62, no. 12, pp. 2931–2940, Dec. 2015.

[10] M. Mercuri *et al.*, "Analysis of an indoor biomedical radar-based system for health monitoring," *IEEE Trans. Microw. Theory Techn.*, vol. 61, no. 5, pp. 2061–2068, May 2013.

[11] C.-S. Lin, S.-F. Chang, C.-C. Chang, and C.-C. Lin, "Microwave human vocal vibration signal detection based on Doppler radar technology," *IEEE Trans. Microw. Theory Techn.*, vol. 58, no. 8, pp. 2299–2306, Aug. 2010.

[12] H. Hong *et al.*, "Time-varying vocal folds vibration detection using a 24 GHz portable auditory radar," *Sensors*, vol. 16, no. 8, p. 1181, 2016.

[13] M. Jiao, G. Lu, X. Jing, S. Li, Y. Li, and J. Wang, "A novel radar sensor for the non-contact detection of speech signals," *Sensors*, vol. 10, no. 5, pp. 4622–4633, 2010.

[14] H. Zhao, Z. Peng, H. Hong, X. Zhu, and C. Li, "A portable 24-GHz auditory radar for non-contact speech sensing with background noise rejection and directional discrimination," in *IEEE MTT-S Int. Microw. Symp. Dig.*, May 2016, pp. 1–4.

[15] C. Gu *et al.*, "Accurate respiration measurement using DC-coupled continuous-wave radar sensor for motion-adaptive cancer radiotherapy," *IEEE Trans. Biomed. Eng.*, vol. 59, no. 11, pp. 3117–3123, Nov. 2012.

[16] C. Gu, R. Li, S. B. Jiang, and C. Li, "A multi-radar wireless system for respiratory gating and accurate tumor tracking in lung cancer radiotherapy," in *Proc. Annu. Int. Conf. IEEE Eng. Med. Biol. Soc. (EMBC)*, Aug. 2011, pp. 417–420.

[17] C. Gu and C. Li, "From tumor targeting to speech monitoring: Accurate respiratory monitoring using medical continuous-wave radar sensors," *IEEE Microw. Mag.*, vol. 15, no. 4, pp. 66–76, Jun. 2014.

[18] J. A. Rice, C. Li, C. Gu, and J. Hernandez, "A wireless multifunctional radar-based displacement sensor for structural health monitoring," *Proc. SPIE*, vol. 7981, p. 79810K, Apr. 2010.

[19] S. Guan, J. A. Rice, C. Li, Y. Li, and G. Wang, "Structural displacement measurements using DC coupled radar with active transponder," *Struct. Control Health Monitor.*, Jan. 2016, to be published.

[20] V. C. Chen and H. Ling, "Joint time-frequency analysis for radar signal and image processing," *IEEE Signal Process. Mag.*, vol. 16, no. 2, pp. 81–93, Mar. 1999.

[21] V. C. Chen, "Analysis of radar micro-Doppler with time-frequency transform," in *Proc. 10th IEEE Workshop Statist Signal Array Process.*, Aug. 2000, pp. 463–466.

[22] Y. Wang and A. E. Fathy, "Micro-Doppler signatures for intelligent human gait recognition using a UWB impulse radar," in *Proc. IEEE Int. Symp. Antennas Propag. (APSURSI)*, Jul. 2011, pp. 2103–2106.

[23] J. Lien *et al.*, "Soli: Ubiquitous gesture sensing with millimeter wave radar," *ACM Trans. Graph.*, vol. 35, no. 4, pp. 1–19, Jul. 2016.

[24] A. Naqvi, S.-T. Yang, and H. Ling, "Investigation of Doppler features from wind turbine scattering," *IEEE Antennas Wireless Propag. Lett.*, vol. 9, pp. 485–488, 2010.

[25] N. Whitelonis, S.-T. Yang, and H. Ling, "Application of near-field to far-field transformation to Doppler features from wind turbine scattering," *IEEE Trans. Antennas Propag.*, vol. 60, no. 3, pp. 1660–1665, Mar. 2012.

[26] J.-M. Muñoz-Ferreras, Z. P. Peng, Y. Tang, R. Gómez-García, D. Liang, and C. Li, "Short-range Doppler-radar signatures from industrial wind turbines: Theory, simulations, and measurements," *IEEE Trans. Instrum. Meas.*, vol. 65, no. 9, pp. 2108–2119, Sep. 2016.

[27] P. Suresh, T. Thayaparan, T. Obulesu, and K. Venkataramaniah, "Extracting micro-Doppler radar signatures from rotating targets using Fourier–Bessel transform and time–frequency analysis," *IEEE Trans. Geosci. Remote Sens.*, vol. 52, no. 6, pp. 3204–3210, Jun. 2014.

[28] A. Koelpin, F. Lurz, S. Linz, S. Mann, C. Will, and S. Lindner, "Six-port based interferometry for precise radar and sensing applications," *Sensors*, vol. 16, no. 10, p. 1556, 2016.

[29] N. Pohl, T. Jaeschke, and K. Aufinger, "An ultra-wideband 80 GHz FMCW radar system using a SiGe bipolar transceiver chip stabilized by a fractional-N PLL synthesizer," *IEEE Trans. Microw. Theory Techn.*, vol. 60, no. 3, pp. 757–765, Mar. 2012.

[30] G. Vinci, S. Lindner, F. Barbon, R. Weigel, and A. Koelpin, "Promise of a better position," *IEEE Microw. Mag.*, vol. 13, no. 7, pp. S41–S49, Dec. 2012.

[31] A. Anghel, G. Vasile, R. Cacoveanu, C. Ioana, and S. Ciochina, "Short-range wideband FMCW radar for millimetric displacement measurements," *IEEE Trans. Geosci. Remote Sens.*, vol. 52, no. 9, pp. 5633–5642, Sep. 2014.

[32] S. Jardak *et al.*, "Detection and localization of multiple short range targets using FMCW radar signal," in *Proc. Global Symp. Millim. Waves (GSMM), ESA Workshop Millime.-Wave Technol. Appl.*, Jun. 2016, pp. 1–4.

[33] J. Li and P. Stoica, *MIMO Radar Signal Processing*. Hoboken, NJ, USA: Wiley, 2009.

[34] T. Jaeschke, C. Bredendiek, and N. Pohl, "A 240 GHz ultra-wideband FMCW radar system with on-chip antennas for high resolution radar imaging," in *IEEE MTT-S Int. Microw. Symp. Dig.*, Jun. 2013, pp. 1–4.

[35] N. Pohl *et al.*, "Radar measurements with micrometer accuracy and nanometer stability using an ultra-wideband 80 GHz radar system," in *Proc. IEEE Top. Conf. Wireless Sensors Sensor Netw. (WiSNet)*, Jan. 2013, pp. 31–33.

[36] D. Zito, D. Pepe, M. Mincica, and F. Zito, "A 90nm CMOS SoC UWB pulse radar for respiratory rate monitoring," in *IEEE Int. Solid-State Circuits Conf. Dig. Tech. Papers (ISSCC)*, Feb. 2011, pp. 40–41.

[37] D. Zito *et al.*, "SoC CMOS UWB pulse radar sensor for contactless respiratory rate monitoring," *IEEE Trans. Biomed. Circuits Syst.*, vol. 5, no. 6, pp. 503–510, Dec. 2011.

[38] E. C. Fear, J. Bourqui, C. Curtis, D. Mew, B. Docktor, and C. Romano, "Microwave breast imaging with a monostatic radar-based system: A study of application to patients," *IEEE Trans. Microw. Theory Techn.*, vol. 61, no. 5, pp. 2119–2128, May 2013.

[39] C. Zhang, M. J. Kuhn, B. C. Merkl, A. E. Fathy, and M. R. Mahfouz, "Real-time noncoherent UWB positioning radar with millimeter range accuracy: Theory and experiment," *IEEE Trans. Microw. Theory Techn.*, vol. 58, no. 1, pp. 9–20, Jan. 2010.

[40] Y. Wang, Q. Liu, and A. E. Fathy, "CW and pulse–Doppler radar processing based on FPGA for human sensing applications," *IEEE Trans. Geosci. Remote Sens.*, vol. 51, no. 5, pp. 3097–3107, May 2013.

[41] B.-H. Ku *et al.*, "A 77-81-GHz 16-element phased-array receiver with ±50° beam scanning for advanced automotive radars," *IEEE Trans. Microw. Theory Techn.*, vol. 62, no. 11, pp. 2823–2832, Nov. 2014.

[42] J. Hatch, A. Topak, R. Schnabel, T. Zwick, R. Weigel, and C. Waldschmidt, "Millimeter-wave technology for automotive radar sensors in the 77 GHz frequency band," *IEEE Trans. Microw. Theory Techn.*, vol. 60, no. 3, pp. 845–860, Mar. 2012.

[43] H. P. Forstner *et al.*, "A 77GHz 4-channel automotive radar transceiver in SiGe," in *Proc. IEEE Radio Freq. Integr. Circuits Symp.*, Jun. 2008, pp. 233–236.

[44] F. Bauer, X. Wang, W. Menzel, and A. Stelzer, "A 79-GHz radar sensor in LTCC technology using grid array antennas," *IEEE Trans. Microw. Theory Techn.*, vol. 61, no. 6, pp. 2514–2521, Jun. 2013.

[45] M. Klotz and H. Rohling, "24 GHz radar sensors for automotive applications," in *Proc. 13th Int. Conf. Microw., Radar Wireless Commun. (MIKON)*, vol. 1. May 2000, pp. 359–362.

[46] G. Hasenaecker, M. van Delden, T. Jaeschke, N. Pohl, K. Aufinger, and T. Musch, "A SiGe fractional-*N* frequency synthesizer for mm-wave wideband FMCW radar transceivers," *IEEE Trans. Microw. Theory Techn.*, vol. 64, no. 3, pp. 847–858, Mar. 2016.

[47] R. Ebelt *et al.*, "Cooperative indoor localization using 24-GHz CMOS radar transceivers," *IEEE Trans. Microw. Theory Techn.*, vol. 62, no. 9, pp. 2193–2203, Sep. 2014.

[48] P. Hariharan, *Basics of Interferometry*. San Diego, CA, USA: Academic, 2010.

[49] L. Lu, C. Li, and J. A. Rice, "A software-defined multifunctional radar sensor for linear and reciprocal displacement measurement," presented at the IEEE Top. Conf. Wireless Sensors Netw., Phoenix, AZ, USA, Jan. 2011, pp. 16–20.

[50] G. Wang, J. M. Munoz-Ferreras, C. Gu, C. Li, and R. Gomez-Garcia, "Application of linear-frequency-modulated continuous-wave (LFMCW) radars for tracking of vital signs," *IEEE Trans. Microw. Theory Techn.*, vol. 62, no. 6, pp. 1387–1399, Jun. 2014.

[51] Z. Peng *et al.*, "A portable FMCW interferometry radar with programmable low-IF architecture for localization, ISAR imaging, and vital sign tracking," *IEEE Trans. Microw. Theory Techn.*, to be published.

[52] J. D. Taylor, *Introduction to Ultra-Wideband Radar Systems*. Boca Raton, FL, USA: CRC, 1994.

[53] J. D. Taylor, *Ultra-Wideband Radar Technology*. Boca Raton, FL, USA: CRC, 2000.

[54] A. B. Suksmono, E. Bharata, A. A. Lestari, A. G. Yarovoy, and L. P. Ligthart, "Compressive stepped-frequency continuous-wave ground-penetrating radar," *IEEE Geosci. Remote Sens. Lett.*, vol. 7, no. 4, pp. 665–669, Oct. 2010.

[55] H. M. Jol, *Ground Penetrating Radar Theory and Applications*. Amsterdam, The Netherlands: Elsevier, 2008.

[56] P. Karsmakers, T. Croonenborghs, M. Mercuri, D. Schreurs, and P. Leroux, "Automatic in-door fall detection based on microwave radar measurements," in *Proc. 9th Eur. Radar Conf. (EuRAD)*, Oct. 2012, pp. 202–205.

[57] M. Mercuri, D. Schreurs, and P. Leroux, "SFCW microwave radar for in-door fall detection," in *Proc. IEEE Top. Conf. Biomed. Wireless Technol., Netw., Sens. Syst. (BioWireleSS)*, Jan. 2012, pp. 53–56.

[58] L. Ren, H. Wang, K. Naishadham, Q. Liu, and A. E. Fathy, "Non-invasive detection of cardiac and respiratory rates from stepped frequency continuous wave radar measurements using the state space method," in *IEEE MTT-S Int. Microw. Symp. Dig.*, May 2015, pp. 1–4.

[59] C. Li, J. Lin, and Y. Xiao, "Robust overnight monitoring of human vital signs by a non-contact respiration and heartbeat detector," in *Proc. 28th Annu. Int. Conf. IEEE Eng. Med. Biol. Soc. (EMBS)*, Aug. 2006, pp. 2235–2238.

[60] W. Massagram, V. M. Lubecke, and O. Boric-Lubecke, "Microwave non-invasive sensing of respiratory tidal volume," in *Proc. Annu. Int. Conf. IEEE Eng. Med. Biol. Soc. (EMBC)*, Dec. 2009, pp. 4832–4835.

[61] A. D. Droitcour *et al.*, "Non-contact respiratory rate measurement validation for hospitalized patients," in *Proc. Annu. Int. Conf. IEEE Eng. Med. Biol. Soc.*, Sep. 2009, pp. 4812–4815.

[62] N. Hafner, I. Mostafanezhad, V. M. Lubecke, O. Boric-Lubecke, and A. Host-Madsen, "Non-contact cardiopulmonary sensing with a baby monitor," in *Proc. 29th Annu. Int. Conf. IEEE Eng. Med. Biol. Soc.*, Aug. 2007, pp. 2300–2302.

[63] Y. Yan, C. Li, X. Yu, M. D. Weiss, and J. Lin, "Verification of a non-contact vital sign monitoring system using an infant simulator," in *Proc. Annu. Int. Conf. IEEE Eng. Med. Biol. Soc.*, Sep. 2009, pp. 4836–4839.

[64] K.-M. Chen, D. Misra, H. Wang, H.-R. Chuang, and E. Postow, "An X-band microwave life-detection system," *IEEE Trans. Biomed. Eng.*, vol. BME-33, no. 7, pp. 697–701, Jul. 1986.

[65] H.-R. Chuang, Y. F. Chen, and K.-M. Chen, "Automatic clutter-canceler for microwave life-detection systems," *IEEE Trans. Instrum. Meas.*, vol. 40, no. 4, pp. 747–750, Aug. 1991.

[66] K.-M. Chen, Y. Huang, J. Zhang, and A. Norman, "Microwave life-detection systems for searching human subjects under earthquake rubble or behind barrier," *IEEE Trans. Biomed. Eng.*, vol. 47, no. 1, pp. 105–114, Jan. 2000.

[67] C. Li, C. Gu, R. Li, and S. B. Jiang, "Radar motion sensing for accurate tumor tracking in radiation therapy," in *Proc. IEEE 12th Annu. Wireless Microw. Technol. Conf. (WAMICON)*, Apr. 2011, pp. 1–6.

[68] C. Gu, Z. Peng, and C. Li, "High-precision motion detection using low-complexity Doppler radar with digital post-distortion technique," *IEEE Trans. Microw. Theory Techn.*, vol. 64, no. 3, pp. 961–971, Mar. 2016.

[69] National Research Council, *Microbial Status and Genetic Evaluation of Mice and Rats: Proceedings of the 1999 US/Japan Conference*. Washington, DC, USA: Nat. Academies Press, 2000.

[70] C. Li and J. Lin, "Non-contact measurement of periodic movements by a 22–40GHz radar sensor using nonlinear phase modulation," in *IEEE MTT-S Int. Microw. Symp. Dig.*, Jun. 2007, pp. 579–582.

[71] T.-Y. Huang, J. Lin, and L. Hayward, "Non-invasive measurement of laboratory rat's cardiorespiratory movement using a 60-GHz radar and nonlinear Doppler phase modulation," in *Proc. IEEE MTT-S Int. Microw. Workshop Ser. RF Wireless Technol. Biomed. Healthcare Appl.*, Sep. 2015, pp. 83–84.

[72] T.-Y. J. Kao, Y. Yan, T.-M. Shen, A. Y.-K. Chen, and J. Lin, "Design and analysis of a 60-GHz CMOS Doppler micro-radar system-in-package for vital-sign and vibration detection," *IEEE Trans. Microw. Theory Techn.*, vol. 61, no. 4, pp. 1649–1659, Apr. 2013.

[73] T. Y. Huang, L. Hayward, and J. Lin, "Adaptive harmonics comb notch digital filter for measuring heart rate of laboratory rat using a 60-GHz radar," in *IEEE MTT-S Int. Microw. Symp. Dig.*, May 2016, pp. 1–4.

[74] F. K. Wang *et al.*, "A novel vital-sign sensor based on a self-injection-locked oscillator," *IEEE Trans. Microw. Theory Techn.*, vol. 58, no. 12, pp. 4112–4120, Dec. 2010.

[75] F.-K. Wang, T.-S. Horng, K.-C. Peng, J.-K. Jau, J.-Y. Li, and C.-C. Chen, "Single-antenna Doppler radars using self and mutual injection locking for vital sign detection with random body movement cancellation," *IEEE Trans. Microw. Theory Techn.*, vol. 59, no. 12, pp. 3577–3587, Dec. 2011.

[76] A. Singh, S. S. Lee, M. Butler, and V. Lubecke, "Activity monitoring and motion classification of the lizard *Chamaeleo jacksonii* using multiple Doppler radars," in *Proc. Annu. Int. Conf. IEEE Eng. Med. Biol. Soc.*, Aug. 2012, pp. 4525–4528.

[77] A. Singh, N. Hafner, V. Lubecke, and M. Butler, "A data efficient method for characterization of chameleon tongue motion using Doppler radar," in *Proc. Annu. Int. Conf. IEEE Eng. Med. Biol. Soc.*, Aug. 2012, pp. 574–577.

[78] N. Hafner, J. C. Drazen, and V. M. Lubecke, "Fish heart rate monitoring by body-contact Doppler radar," *IEEE Sensors J.*, vol. 13, no. 1, pp. 408–414, Jan. 2012.

[79] B. Spencer, Jr., S. Cho, and S.-H. Sim, "Wireless monitoring of civil infrastructure comes of age," *Structure Mag.*, vol. 13, pp. 12–16, Oct. 2011.

[80] B. F. Spencer, Jr., M. E. Ruiz-Sandoval, and N. Kurata, "Smart sensing technology: Opportunities and challenges," *Struct. Control Health Monitor.*, vol. 11, no. 4, pp. 349–368, Oct./Dec. 2004.

[81] F. Mohd-Yasin, C. E. Korman, and D. J. Nagel, "Measurement of noise characteristics of MEMS accelerometers," *Solid-State Electron.*, vol. 47, no. 2, pp. 357–360, 2003.

[82] H. H. Nassif, M. Gindy, and J. Davis, "Comparison of laser Doppler vibrometer with contact sensors for monitoring bridge deflection and vibration," *NDT E Int.*, vol. 38, no. 3, pp. 213–218, 2005.

[83] M. Pieraccini, M. Fratini, F. Parrini, and C. Atzeni, "Dynamic monitoring of bridges using a high-speed coherent radar," *IEEE Trans. Geosci. Remote Sens.*, vol. 44, no. 11, pp. 3284–3288, Nov. 2006.

[84] M. Pieraccini, M. Fratini, F. Parrini, C. Atzeni, and G. Bartoli, "Interferometric radar vs. accelerometer for dynamic monitoring of large structures: An experimental comparison," *NDT E Int.*, vol. 41, no. 4, pp. 258–264, 2008.

[85] M. Fratini, F. Parrini, M. Pieraccini, C. Borri, and C. Atzeni, "Structural oscillation modes identification by applying controlled loads and using microwave interferometry," *NDT E Int.*, vol. 42, no. 8, pp. 748–752, 2009.

[86] J. A. Rice, C. Gu, C. Li, and S. Guan, "A radar-based sensor network for bridge displacement measurements," *Proc. SPIE*, vol. 8345, p. 83450I, Apr. 2012.

[87] Y. Kim and H. Ling, "Human activity classification based on micro-Doppler signatures using a support vector machine," *IEEE Trans. Geosci. Remote Sens.*, vol. 47, no. 5, pp. 1328–1337, May 2009.

[88] V. C. Chen and H. Ling, *Time-Frequency Transforms for Radar Imaging and Signal Analysis*. Norwood, MA, USA: Artech House, 2002.

[89] V. C. Chen, F. Li, S.-S. Ho, and H. Wechsler, "Micro-Doppler effect in radar: Phenomenon, model, and simulation study," *IEEE Trans. Aerosp. Electron. Syst.*, vol. 42, no. 1, pp. 2–21, Jan. 2006.

[90] G. Wang, C. Gu, T. Inoue, and C. Li, "A hybrid FMCW-interferometry radar for indoor precise positioning and versatile life activity monitoring," *IEEE Trans. Microw. Theory Techn.*, vol. 62, no. 11, pp. 2812–2822, Nov. 2014.

[91] Q. Wan, Y. Li, C. Li, and R. Pal, "Gesture recognition for smart home applications using portable radar sensors," in *Proc. 36th Annu. Int. Conf. IEEE Eng. Med. Biol. Soc.*, Aug. 2014, pp. 6414–6417.

[92] P. Molchanov, S. Gupta, K. Kim, and K. Pulli, "Short-range FMCW monopulse radar for hand-gesture sensing," in *Proc. IEEE Radar Conf. (RadarCon)*, May 2015, pp. 1491–1496.

[93] C. C. Ciang, J.-R. Lee, and H.-J. Bang, "Structural health monitoring for a wind turbine system: A review of damage detection methods," *Meas. Sci. Technol.*, vol. 19, no. 12, 2008, Art. no. 122001.

[94] R. W. Hyers, J. G. McGowan, K. L. Sullivan, J. F. Manwell, and B. C. Syrett, "Condition monitoring and prognosis of utility scale wind turbines," *Energy Mater.*, vol. 1, no. 3, pp. 187–203, Sep. 2006.

[95] M. A. Rumsey and J. A. Paquette, "Structural health monitoring of wind turbine blades," *Proc. SPIE*, vol. 6933, p. 69330E, Apr. 2008.

[96] H.-L. Fu, K.-C. Fan, Y.-J. Huang, and M.-K. Hu, "Innovative optical scanning technique and device for three-dimensional full-scale measurement of wind-turbine blades," *Opt. Eng.*, vol. 53, no. 12, 2014, Art. no. 122411.

[97] L. Glavind, I. S. Olesen, B. F. Skipper, and M. Kristensen, "Fiber-optical grating sensors for wind turbine blades: A review," *Opt. Eng.*, vol. 52, no. 3, Mar. 2013, Art. no. 030901.

[98] J. Wang, X. Wang, L. Chen, J. Huangfu, C. Li, and L. Ran, "Noncontact distance and amplitude-independent vibration measurement based on an extended DACM algorithm," *IEEE Trans. Instrum. Meas.*, vol. 63, no. 1, pp. 145–153, Jan. 2014.

[99] S. Mann, F. Lurz, R. Weigel, and A. Koelpin, "A high-sensitivity radar system featuring low weight and power consumption," *IEEE Microw. Mag.*, vol. 16, no. 2, pp. 99–105, Mar. 2015.

[100] C.-H. Chao, T.-W. Hsu, and C.-H. Tseng, "Giving Doppler more bounce: A 5.8 GHz microwave high-sensitivity Doppler radar system," *IEEE Microw. Mag.*, vol. 17, no. 1, pp. 52–57, Jan. 2016.

[101] D. A. Ausherman, A. Kozma, J. L. Walker, H. M. Jones, and E. C. Poggio, "Developments in radar imaging," *IEEE Trans. Aerosp. Electron. Syst.*, vol. AES-20, no. 4, pp. 363–400, Jul. 1984.

[102] J. L. Walker, "Range-Doppler imaging of rotating objects," *IEEE Trans. Aerosp. Electron. Syst.*, vol. AES-16, no. 1, pp. 23–52, Jan. 1980.

[103] F. Berizzi, E. D. Mese, M. Diani, and M. Martorella, "High-resolution ISAR imaging of maneuvering targets by means of the range instantaneous Doppler technique: Modeling and performance analysis," *IEEE Trans. Image Process.*, vol. 10, no. 12, pp. 1880–1890, Dec. 2001.

[104] Z. Peng, J.-M. Muñoz-Ferreras, R. Gómez-García, and C. Li, "FMCW radar fall detection based on ISAR processing utilizing the properties of RCS, range, and Doppler," in *IEEE MTT-S Int. Microw. Symp. Dig.*, May 2016, pp. 1–3.

[105] C. Zheng, T. Hu, S. Qiao, Y. Sun, J. Huangfu, and L. Ran, "Doppler bio-signal detection based time-domain hand gesture recognition," in *Proc. IEEE MTT-S Int. Microw. Workshop Ser. RF Wireless Technol. Biomed. Healthcare Appl.*, Dec. 2013, p. 3.

[106] T. Fan *et al.*, "Wireless hand gesture recognition based on continuous-wave Doppler radar sensors," *IEEE Trans. Microw. Theory Techn.*, vol. 64, no. 11, pp. 4012–4020, Nov. 2016.

Changzhi Li (S'06–M'09–SM'13) received the B.S. degree in electrical engineering from Zhejiang University, Hangzhou, China, in 2004, and the Ph.D. degree in electrical engineering from the University of Florida, Gainesville, FL, USA, in 2009.

From 2007 to 2009, he was with Alereon Inc., Austin, TX, USA, and Coherent Logix Inc., Austin, where he was involved in ultrawideband transceivers and software-defined radio, respectively. He joined Texas Tech University, Lubbock, TX, USA, as an Assistant Professor in 2009, and then became an Associate Professor in 2014. His current research interests include biomedical applications of microwave technology, wireless sensors, and RF/analog circuits.

Dr. Li was a recipient of the IEEE Sensors Council Early Career Technical Achievement Award in 2016, the ASEE Frederick Emmons Terman Award in 2014, the IEEE-HKN Outstanding Young Professional Award in 2014, the NSF Faculty Early CAREER Award in 2013, the IEEE MTT-S Graduate Fellowship Award in 2008, and nine Best Conference/Student Paper Awards as an author/advisor in IEEE-sponsored conferences. He is an Associate Editor of the IEEE Transactions on Circuits and Systems—I: Regular Papers. He served as an Associate Editor of the IEEE Transactions on Circuits and Systems—II: Express Briefs in 2014 and 2015. He served as a TPC Co-Chair of the IEEE Wireless and Microwave Technology Conference in 2012 and 2013.

Zhengyu Peng (S'15) received the B.S. and M.Sc. degrees in electrical engineering from Zhejiang University, Hangzhou, China, in 2011 and 2014, respectively. He is currently pursuing the Ph.D. degree in electrical engineering at Texas Tech University, Lubbock, TX, USA.

His current research interests include antennas, microwave circuits, and biomedical applications of microwave/RF circuits and systems.

Mr. Peng was a recipient of the 2016 IEEE Microwave Theory and Techniques Society Graduate Fellowship, Third Place of the Student Design Competition for high-sensitivity radar in the 2015 IEEE International Microwave Symposium, and the Excellent Demo Track Presentation Award in 2016 IEEE Radio and Wireless Week. He is a reviewer for the IEEE Transactions on Circuits and Systems—II: Express Briefs and the *International Journal of Electronics and Communications*.

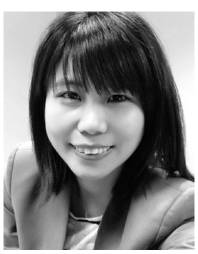

Tien-Yu Huang (S'13) received the B.S. degree in electrical engineering and M.S. degree in communication engineering from Tatung University, Taipei, Taiwan, in 2009 and 2010, respectively. She is currently pursuing the Ph.D. degree in electrical and computer engineering at the University of Florida, Gainesville, FL, USA.

Her current research interests include biomedical application of Doppler radar sensors, RF integrated circuit design, and carbon nanotube aerogels-based hydrogen sensors.

Ms. Huang is a Student Member of the IEEE Microwave Theory and Techniques Society (IEEE MTT-S). She was the First-Place recipient of the Best Student Paper Award in 2015 IEEE MTT-S IMWS-Bio, the Second-Place recipient of the Student Paper Competition in 2016 IEEE RWW BioWireleSS, and a Finalist in the IMS2016 Student Paper Competition. She and her colleague won Third Place of the Student Design Competition for high-sensitivity radar at the 2014 IEEE MTT-S International Microwave Symposium.

Tenglong Fan received the B.S. degree from Zhejiang University, Hangzhou, China, in 2014, where he is currently pursuing the master's degree at the Laboratory of Applied Research on Electromagnetics.

His current research interests include RF systems, microwave circuits, and wireless detection.

Fu-Kang Wang (S'10–M'13) was born in Kaohsiung, Taiwan, in 1985. He received the B.S.E.E., M.S.E.E., and Ph.D. degrees from National Sun Yat-sen University (NSYSU), Kaohsiung, in 2007, 2009, and 2013, respectively.

He was a Post-Doctoral Research Fellow with NSYSU in 2014, and a Visiting Researcher with IMEC, Leuven, Belgium, in 2015. Since 2016, he has been with the EM Wave Group, Department of Electrical Engineering, NSYSU, where he is currently an Assistant Professor. He holds five U.S. patents about radar systems. His current research interests include RF sensing techniques.

Dr. Wang was the recipient of the Outstanding Doctoral Dissertation Award from NSYSU in 2013 and the Post-Doctoral Research Abroad Program Fellowship by the Ministry of Science and Technology, Taiwan, in 2014.

Tzyy-Sheng Horng (S'88–M'92–SM'05–F'16) was born in Taichung, Taiwan, in 1963. He received the B.S.E.E. degree from National Taiwan University, Taipei, Taiwan, in 1985, and the M.S.E.E. and Ph.D. degrees from the University of California, Los Angeles, CA, USA, in 1990 and 1992, respectively.

Since 1992, he has been with the Department of Electrical Engineering, National Sun Yat-sen University, Kaohsiung, Taiwan, where he was the Director of the Telecommunication Research and Development Center from 2003 to 2008 and the Director of the Institute of Communications Engineering from 2004 to 2007, and is currently a Distinguished Professor. He has authored or co-authored over 240 technical publications in refereed journal and conference proceedings, mostly in IEEE publications. He holds over ten U.S. patents. His current research interests include RF and microwave ICs and components, RF signal integrity for wireless system-in-package, digitally assisted RF technologies, and green radios for cognitive sensors and Doppler radars.

Dr. Horng is currently a member of the IEEE MTT-S Technical Committees MTT-10 and MTT-20. He was the recipient of the 1996 Young Scientist Award from the International Union of Radio Science, the 1998 Industry-Education Cooperation Award from the Ministry of Education, Taiwan, the 2011 Chair Professorship awarded by Advanced Semiconductor Engineering, Inc., the 2012 Outstanding Research Award from National Sun Yat-sen University, and the 2016 Outstanding Research Award from the Ministry of Science and Technology, Taiwan. He was the Founder Chair of the IEEE MTT-S Tainan Chapter in 2009, and an Associate Editor of the IEEE Transactions on Microwave Theory and Techniques from 2012 to 2015. He served on several Technical Program Committees of international conferences including the International Association of Science and Technology for Development, the International Conference on Wireless and Optical Communications, the IEEE Region 10 International Technical Conference, the IEEE International Workshop on Electrical Design of Advanced Packaging and Systems, the Asia-Pacific Microwave Conference, the IEEE Radio and Wireless Symposium, and the Electronic Components and Technology Conference. He has also served on the Project Review Board in the Programs of Communications Engineering and Microelectronics Engineering at the Ministry of Science and Technology, Taiwan.

José-María Muñoz-Ferreras (M'15) received the degree in telecommunication engineering and Ph.D. degree in electrical and electronic engineering from the Polytechnic University of Madrid, Madrid, Spain, in 2004 and 2008, respectively.

He is currently an Associate Professor with the Department of Signal Theory and Communications, University of Alcalá, Alcalá de Henares, Spain. His current research interests include radar signal processing, advanced radar systems and concepts, and microwave/RF circuits and systems, with a focus on high-resolution inverse synthetic aperture radar images, and the design and validation of radar systems for short-range applications.

Dr. Muñoz-Ferreras serves as a member of the Technical Review Board of the IEEE International Geoscience and Remote Sensing Symposium, the IEEE Radar Conference, and the European Radar Conference. He is a reviewer for several IEEE and IET publications.

Roberto Gómez-García (S'02–M'06–SM'11) was born in Madrid, Spain, in 1977. He received the degree in telecommunication engineering and Ph.D. degree in electrical and electronic engineering from the Polytechnic University of Madrid, Madrid, in 2001 and 2006, respectively.

Since 2006, he has been an Associate Professor with the Department of Signal Theory and Communications, University of Alcalá, Alcalá de Henares, Madrid. He has been, for several research stays, with the C2S2 Department, XLIM Research Institute, University of Limoges, Limoges, France, the Telecommunications Institute, University of Aveiro, Aveiro, Portugal, the U.S. Naval Research Laboratory, Microwave Technology Branch, Washington, DC, USA, and Purdue University, West Lafayette, IN, USA. His current research interests include the design of fixed/tunable high-frequency filters and multiplexers in planar, hybrid, and monolithic microwave-integrated circuit technologies, multifunction circuits and systems, and software-defined radio and radar architectures for telecommunications, remote sensing, and biomedical applications.

Dr. Gómez-García serves as a member of the Technical Review Board for several IEEE and EuMA conferences, the IEEE MTT-S Filters and Passive Components (MTT-8), the IEEE MTT-S Biological Effect and Medical Applications of RF and Microwave (MTT-10), the IEEE MTT-S Wireless Communications (MTT-20), and the IEEE CAS-S Analog Signal Processing Technical Committees. He was a recipient of the 2016 IEEE Microwave Theory and Techniques Society (MTT-S) Outstanding Young Engineer Award. From 2012 to 2015, he was an Associate Editor of the IEEE TRANSACTIONS ON CIRCUITS AND SYSTEMS—I: REGULAR PAPERS. He was a Guest Editor of the 2013 IEEE JOURNAL ON EMERGING AND SELECTED TOPICS IN CIRCUITS AND SYSTEMS "Special Issue on Advanced Circuits and Systems for CR/SDR Applications," the *IET Microwaves, Antennas, and Propagation* 2013 "Special Issue on Advanced Tunable/Reconfigurable and Multifunction RF/Microwave Filtering Devices," and *IEEE Microwave Magazine* 2014 "Special Issue on Recent Trends on RF/Microwave Tunable Filter Design." He is currently an Associate Editor of the IEEE TRANSACTIONS ON MICROWAVE THEORY AND TECHNIQUES and the *IET Microwaves, Antennas, and Propagation*, and a Senior Editor of the IEEE JOURNAL ON EMERGING AND SELECTED TOPICS IN CIRCUITS AND SYSTEMS. He is also a reviewer for several IEEE, IET, EuMA, and Wiley journals.

Lixin Ran received the B.S., M.S., and Ph.D. degrees from Zhejiang University, Hangzhou, China, in 1991, 1994, and 1997, respectively.

He was an Assistant Professor in 1997, an Associate Professor in 1999, and a Full Professor in 2004 with the Department of Information and Electronics Engineering, Zhejiang University, where he is currently the Director of the Laboratory of Applied Research on Electromagnetics. In 2005, 2009, and 2012, he visited the Massachusetts Institute of Technology, Cambridge, MA, USA, as a Visiting Scientist. He has co-authored over 120 research papers published in peer-reviewed journals, and holds over 30 licensed patents. His current research interests include new concept antennas, radio-aware sensing and imaging, radio frequency, microwave and terahertz systems, and artificial active media.

Jenshan Lin (S'91–M'94–SM'00–F'10) received the Ph.D. degree in electrical engineering from the University of California, Los Angeles, CA, USA, in 1994.

He was with Lucent Bell Labs, Murray Hill, NJ, USA, from 1994 to 2001, and Agere Systems, Holmdel, NJ, USA, a spin-off company of Lucent Bell Labs, from 2001 to 2003. In 2003, he joined the University of Florida, Gainesville, FL, USA, where he is currently a Professor. Since 2016, he has been with the U.S. National Science Foundation, as a Program Director in Communications, Circuits, and Sensing Systems Program. He has authored or co-authored over 250 technical publications in refereed journals and conference proceedings. He holds 15 U.S. patents. His current research interests include sensors and biomedical applications of microwave and millimeter-wave technologies, wireless power transfer, and wireless communication systems.

Dr. Lin was a recipient of the 1994 UCLA Outstanding Ph.D. Award, the 1997 Eta Kappa Nu Outstanding Young Electrical Engineer Honorable Mention Award, the 2007 IEEE Microwave Theory and Techniques Society N. Walter Cox Award, the 2015 IEEE Wireless Power Transfer Conference Best Paper Award, the 2016 Distinguished Alumnus Award from National Chiao Tung University, Hsinchu, Taiwan, and the 2016 IEEE RFIC Symposium Tina Quach Outstanding Service Award. He was the General Chair of the 2008 RFIC Symposium, the Technical Program Chair of the 2009 Radio and Wireless Symposium, and the General Co-Chair of the 2012 Asia–Pacific Microwave Conference. He served as the Editor-in-Chief of the IEEE TRANSACTIONS ON MICROWAVE THEORY AND TECHNIQUES in 2014–2016.